SAND REPORT

SAND2003-3161
Unlimited Release
Printed October 2003

A Perturbation Expansion Approach to Solving the Electromagnetic Induction Problem in Three Dimensions

Nancy H. Natek and Chester J. Weiss

Prepared by
Sandia National Laboratories
Albuquerque, New Mexico 87185 and Livermore, California 94550

Sandia is a multiprogram laboratory operated by Sandia Corporation, a Lockheed Martin Company, for the United States Department of Energy under Contract DE-AC04-94AL85000.

Issued by Sandia National Laboratories, operated for the United States Department of Energy by Sandia Corporation.

Available to DOE and DOE contractors from
U.S. Department of Energy
Office of Scientific and Technical Information
P.O. Box 62
Oak Ridge, TN 37831

Telephone: (865)576-8401
Facsimile: (865)576-5728
E-Mail: reports@adonis.osti.gov
Online ordering: http://www.doe.gov/bridge

Available to the public from
U.S. Department of Commerce
National Technical Information Service
5285 Port Royal Rd
Springfield, VA 22161

Telephone: (800)553-6847
Facsimile: (703)605-6900
E-Mail: orders@ntis.fedworld.gov
Online order: http://www.ntis.gov/ordering.htm

SAND2003-3161
Unlimited Release
Printed October 2003

A Perturbation Expansion Approach to Solving the Electromagnetic Induction Problem in Three Dimensions

Nancy H. Natek and Chester J. Weiss
Geophysical Technology Department
Sandia National Laboratories
P.O. Box 5800
Albuquerque NM 87185-0750

Harold Tobin
Department of Earth and Environmental Science
New Mexico Tech
Socorro, NM 87801

Abstract

We address the electromagnetic induction problem for fully 3D geologic media and present a solution to the governing Maxwell equations based on a power series expansion. The coefficients in the series are computed using the adjoint method assuming an underlying homogeneous reference model. These solutions are available analytically for point dipole source terms and lead to rapid calculation of the expansion coefficients. First order solutions are presented for a model study in petroleum geophysics composed of a multi-component induction sonde proximal to a fault within a compartmentalized hydrocarbon reservoir.

1 Introduction

The primary objective of geophysical well logging for petroleum is to identify potential reservoir rocks by determining their porosity and permeability, and the nature and volume of fluids present. Water saturation and porosity measurements can provide distinguishing traits of hydrocarbon-bearing formations. Archie (1942) developed empirical equations used in petroleum work to relate resistivity measurements of formations to porosity and water saturation. Formations saturated with oil have a higher resistivity versus formations saturated with saline water; therefore high resistivity readings can denote hydrocarbon-bearing formations.

An induction sonde is a tool designed to measure formation resistivity in boreholes. A multi-component induction sonde consists of a transmitter and receiver coil, typically with offsets of one to three meters. For higher resolutions, multiple transmitter and receiver coils may be used. As the induction sonde is lowered into the borehole and raised at a constant speed, the electromagnetic field produced by the transmitter coil induces eddy currents in conductive formations. These eddy currents in turn induce secondary currents measured in the receiver coil. These secondary currents are direct indicators of the formation conductivity (Telford et al., 1990).

The objective of our modeling study is to investigate the 3D electromagnetic induction problem for a single transmitter/receiver sonde approaching a fault within a hydrocarbon reservoir. In this study, we are interested in calculating the change of the magnetic field strength around the receiver due to a change in conductivity beyond the fault boundary. We calculate these with a perturbation expansion approach for rapid on-site analysis of induction log data and present our results in the frequency and time domains.

2 Sensitivity Computation

For a single medium with a uniform conductivity, we can analytically calculate the electric and magnetic fields around the receiver from point magnetic dipole sources at the transmitter (Ward and Hohmann, 1990). However, for an inhomogeneous case as

in our quarterspace fault model (Figure 1a), the electric and magnetic fields around the receiver cannot be calculated analytically due to the different conductivities of the two media.

A quantity of physical interest is the *sensitivity* $\partial\mathbf{H}/\partial\sigma$, or the variation of the fields at the receiver due to a conductivity perturbation in the media. The magnetic sensitivities at the receiver can be obtained by an approximation (the adjoint method) by solving two boundary value problems (McGillivray et al., 1994). We first calculate the primary electric field $\mathbf{E}$ from a transmitter T, assuming a uniform conductivity σ_0 (Figure 1a). To measure the sensitivity of the x-component of the magnetic field, we then solve for a adjoint electric field $\tilde{\mathbf{E}}$, by placing a fictitious magnetic dipole source located at the receiver R, also pointing in the x-direction, again with uniform conductivity σ_0.

The primary and the adjoint electric fields are then multiplied and integrated over the quarterspace region of the perturbed conductivity, to obtain a numerical value for the sensitivity at the receiver,

$$\left.\frac{\partial H_x}{\partial \sigma}\right|_R = \int_{\Delta\sigma} \tilde{\mathbf{E}} \cdot \mathbf{E}\, dV. \tag{1}$$

The new magnetic field at the receiver is given approximately by a Taylor series expansion:

$$H_x(\sigma) \approx H_x(\sigma_0) + \frac{\partial H_x}{\partial \sigma}\,\Delta\sigma, \tag{2}$$

where $H_x(\sigma_0)$ is the magnetic field calculated analytically over the region of conductivity σ_0 and $\partial H_x/\partial\sigma$ is the sensitivity at the receiver calculated at the receiver with the adjoint method multiplied by the change of conductivity of the quarterspace $\Delta\sigma$. The sensitivities of the y- and z-components of the magnetic field around the receiver are calculated similarly.

3 Algorithm Summary

To design a code to implement this algorithm, we began with a Fortran 77 code developed for the anisotropic wholespace which calculated the magnetic fields and

electric current densities for a homogeneous conductivity in the frequency domain (Moran and Gianzero, 1979).

1. The code was modularized. The driver code and all new modules were written in Fortran 90.

2. We extended the code to calculate the primary and adjoint electric fields and then to calculate the sensitivities for a quarterspace fault model. The integration indicated in Eq.(1) was performed with a fourth order extended Simpson algorithm (Press et al., 1992).

3. The integration over the quarterspace region was computed from the corner of the fault boundary to some arbitrary upper limit, y_{max} (where we took $x_{max} = y_{max} = z_{max}$). An adaptive integration algorithm was developed to automatically determine the minimum upper limit necessary to produce convergent results. From the analytic formulas, the electric and magnetic fields decay as

$$E, H \sim \frac{e^{-r/\delta}}{r}, \qquad \delta = \text{skin depth } \sim 500\sqrt{\frac{\rho}{f}}, \tag{3}$$

   where r is the radial distance from the origin, ρ is the resistivity and f is the frequency in hertz. Therefore, the upper limit of the quarterspace integration is frequency dependent. Low frequencies fall off as $\sim 1/r$ while high frequencies fall off rapidly. To automatically determine the upper limit of the region over which to integrate, the sensitivities are considered to have converged when the relative error of for two successive values of the upper limit is less than a user-defined tolerance. This is of practical importance since integration beyond this minimum distance is computationally expensive, increases run time and adds little to the value of the sensitivity.

4. Interpolating y_{max} for intermediate frequencies significantly reduced calculation time. After a series of runs (Figure 2a) with conductivities in the range from 0.01 to 1.0 S/m (Siemens/meter), we found that the upper limit as a function

of frequency generally fell into three regions. For example, for a conductivity of 0.25 S/m the upper limit had the following form:

(1) $0 - 1$ Hz, all sensitivities converged at 220 m,
(2) 1 Hz - 150 kHz, sensitivities converged from $25 - 190$ m,
(3) $>$ 150 kHz, all sensitivities quickly converged at 20 m,

from the fault corner boundary. For frequencies from $0 - 1$ Hz, we began the integrations at 220 m. This reduced the number of iterations from 44 to three and reduced the calculation times by half or more. By plotting a log-log graph of frequency vs. y_{max} (Figure 2b), we found that y_{max} for the intermediate frequencies 1 Hz - 150 kHz could be interpolated with a power law. This also reduced the calculation time significantly.

5. We incorporated an inverse digital filter Fourier transform code (Hanstein, 2003) to examine time domain sensitivities. Instead of using quadratures to compute the inverse Fourier transform of the sensitivities with respect to temporal frequencies ω (Hz)

$$\frac{\partial H_i(t)}{\partial \sigma} = \frac{1}{2\pi} \int_{-\infty}^{\infty} \frac{\partial H_i(\omega)}{\partial \sigma} e^{i\omega t} \, d\omega, \tag{4}$$

we approximate $\partial H_i(t)/\partial \sigma$ multiplied with a linear filter t, by the discretized expression

$$t \, \frac{\partial H_i(t)}{\partial \sigma} = \sum_{j=1}^{N} w_j \, \frac{\partial H_i(\omega_j)}{\partial \sigma}. \tag{5}$$

In Eq. (5), the filter coefficients w_j and frequencies ω_j are computed by a least squares fit to known transform pairs, similar to the algorithms described in Anderson (1975) and Guptasarma and Singh (1997) for Hankel transforms.

4 Sensitivity Results

For the quarterspace fault model (Figure 1a), sensitivities were calculated for tool locations above and below the fault boundary. Receiver locations at 0, 30, 45 and 60 degrees respectively from the vertical z-axis were used with a one-meter offset

between the transmitter and the receiver (Figure 1b). For these cases, we used the adjoint method by calculating with a z-magnetic directed dipole at the transmitter and with a x-directed magnetic dipole at the receiver.

Figure 3 shows the frequency domain sensitivity plots above (a) and below (b) the fault boundary for four different tool locations. We find that the values of sensitivities peak around 100 kHz, and approach zero for very low or very high frequencies. The peak values for each tool location increased as the sonde was rotated more towards the horizontal (i.e. the y-axis).

Figure 4 shows the time domain sensitivity plots above (a) and below (b) the fault boundary over a dynamic range of four decades of the instrument strength. The cusps at $t < 20\ \mu s$ indicate a sign change in $\partial H_x/\partial\sigma$. Note that the magnitude of the perturbation covers four decades in signal strength. Note, also, that the effect of the quarterspace is more clearly discerned in the frequency domain (Figure 3) as expressed by the magnitude of the peak amplitude of the sensitivities.

5 Conclusions

By using fast, closed-form analytic formulae for the uniform wholespace, we have been able to investigate cases where the conductivity is not homogeneous by using a perturbation expansion approach. With this method we are able to obtain good values of the sensitivities. We find that we do not need to integrate very far into region beyond the fault boundary as the fields fall off rapidly and the sensitivity estimates converge very quickly. By employing an adaptive integration algorithm, we can automatically determine the upper limit of the region over which to integrate and significantly reduced calculation time by interpolating y_{max} for intermediate frequencies. Sensitivities calculated in the frequency domain for a quarterspace fault model with tool locations near the fault corner boundary show peak values around 100 kHz. The peak value for each tool location increases with the angle of the receiver measured with respect to the z-direction (the direction of the oscillating magnetic dipole associated with the transmitter). The effect of the quarterspace is more clearly discerned

in the frequency domain as the magnitude of the peak amplitude.

Further worthwhile investigations include: (1) calculating sensitivities for designated tool locations around the quarterspace to distinguish corner effects; (2) comparing sensitivities computed with the adjoint method with 3D finite difference results to determine the range of the change of conductivity; (3) calculating sensitivities for cases with multiple non-interacting regions of different conductivities and (4) calculating higher order derivatives in the Taylor series expansion using the adjoint method. Several of these studies are planned for continuing work for a master's thesis.

Acknowledgements

The authors wish to thank Tilman Hanstein of KMS Technologies for the use of his inverse digital filter Fourier transform code and the Natural Gas and Oil Technology Partnership (NGOTP) for supporting this work. NHN would like to thank the High Performance Computing Center at the University of New Mexico for the use of its computational resources and for technical support.

References

Anderson, W.L., 1975, *Improved digital filters for evaluation Fourier and Hankel transform integrals*, USGS Report No. USGS-GD-75-012.

Archie, G.E., 1942, *The electric resistivity log as an aid in determining some reservoir characteristics*, Trans. AIME **146**, p. 54-62.

Guptasarma, D., and B. Singh, 1997, *New digital linear filters for Hankel and J_0 and J_1 transforms*, Geophys. Prosp. **45**, p. 745-762.

Hanstein, T., 2003, private communication and contributed code.

Moran, J.H., and Gianzero, S., 1979, *Effects of formation anisotropy on resistivity-logging measurements, Geophysics* **44**, p. 1266-1286.

McGillivray, P.R., D.W. Oldenburg, R.G. Ellis and Habashy, T.M., 1994, *Calculation of sensitivities for the frequency domain electromagnetic problem*, Geophysical Journal International **116**, p. 1-4.

Press, W.H., Teukolsky, S.A., Vettering, W.T., and Flannery, B.P., 1992, *Numerical Recipes in Fortran*, 2 ed., Cambridge University Press, 963 p.

Telford, W.M., Geldart, L.P., and R.E. Sheriff, 1990, *Applied Geophysics*, 2nd Ed., Cambridge University Press, 770 p.

Ward, S.H., and G.W. Hohmann, 1990, *Electromagnetic theory for geophysical applications in electromagnetic Methods in Applied Geophysics*, ed. M.N. Nabighian, Society of Exploration Geophysics, Tulsa, Oklahoma, 513 p.

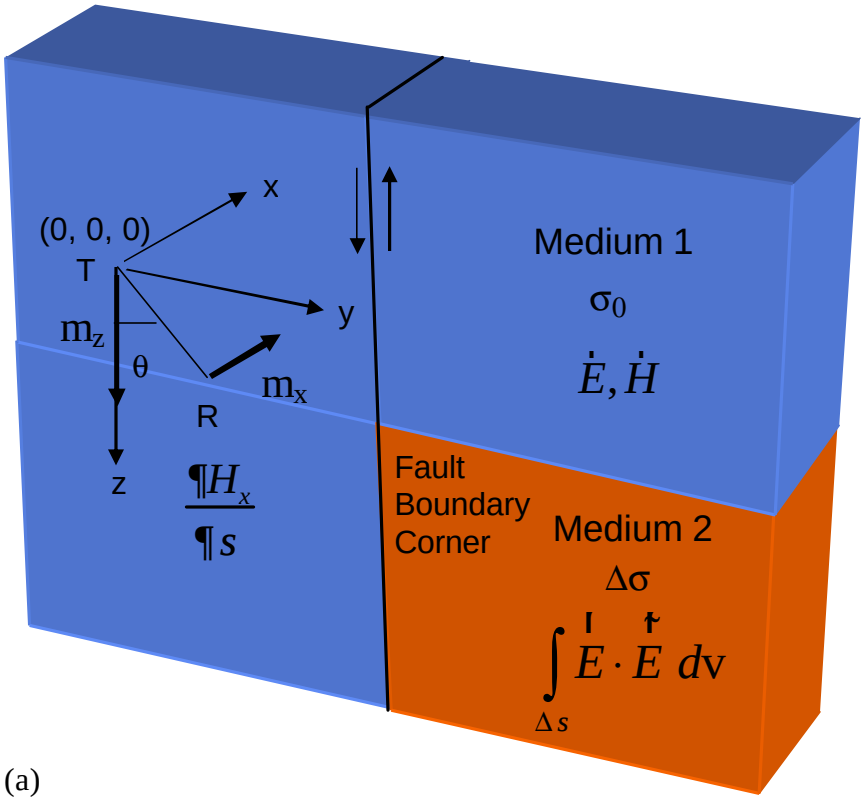

(a)

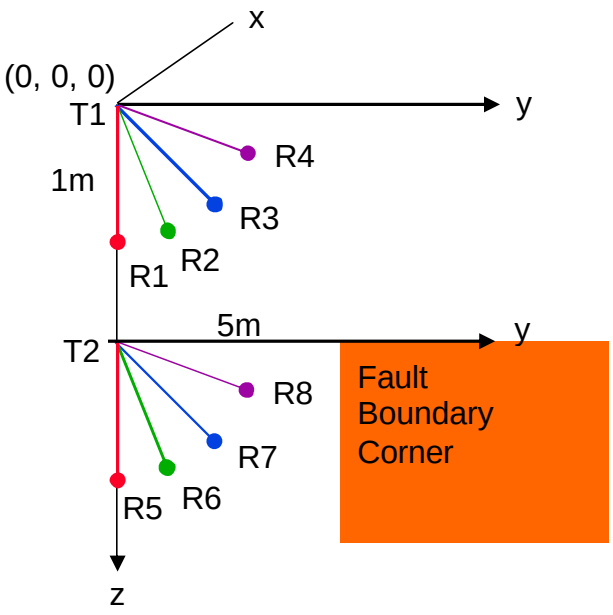

(b)

Figure 1: (a) The quarterspace fault model. (b) Sensitivities are calculated for tool locations above and below the fault boundary and receivers are located at 0, 30, 45, and 60 degrees respectively from the vertical *z*-direction.

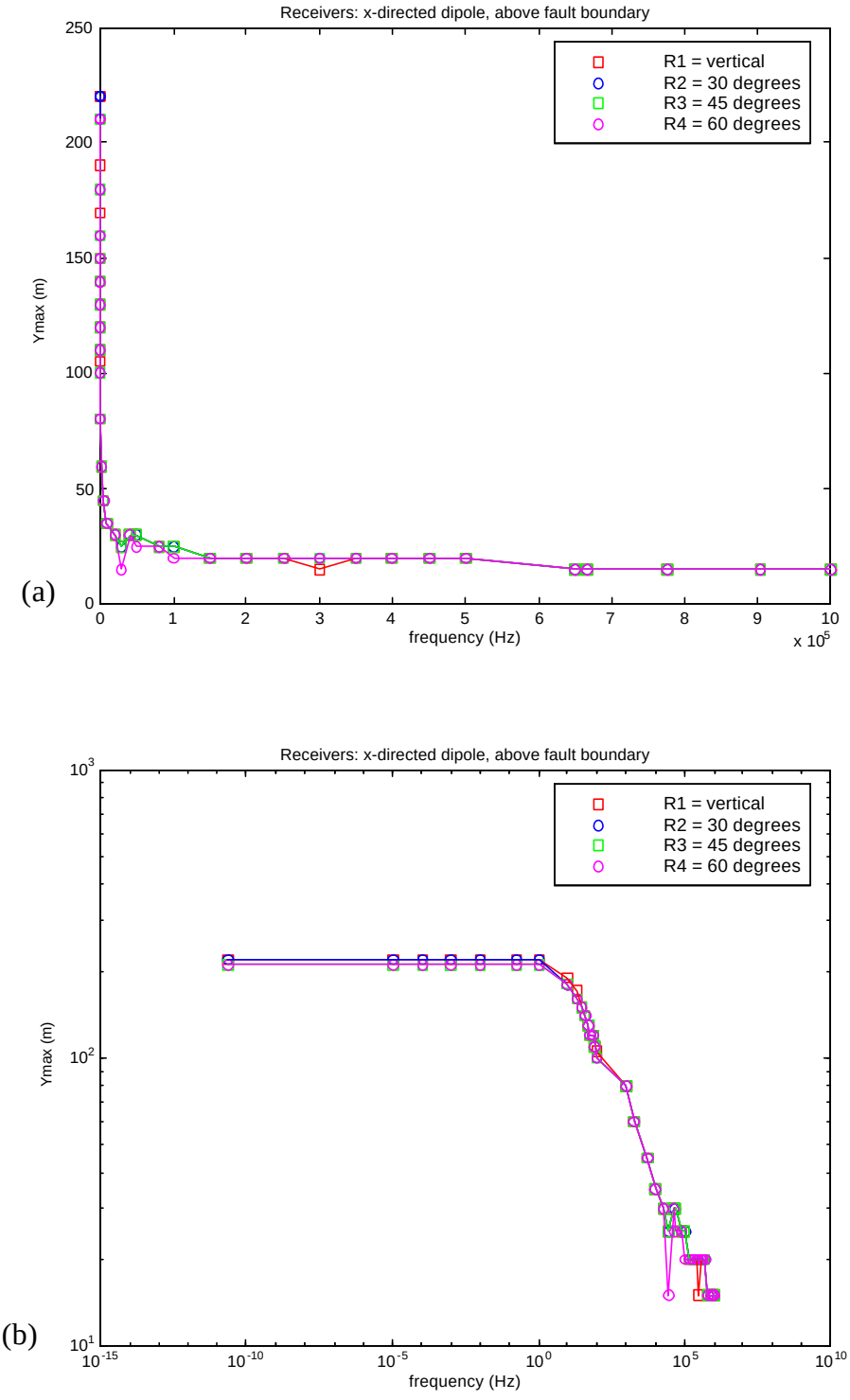

Figure 2: (a) Convergence plot of sensitivities above the fault boundary with a *z*-directed magnetic dipole at the transmitter and a *x*-directed magnetic dipole at the receiver. (b) Convergence plot of sensitivities plotted as a log-log graph.

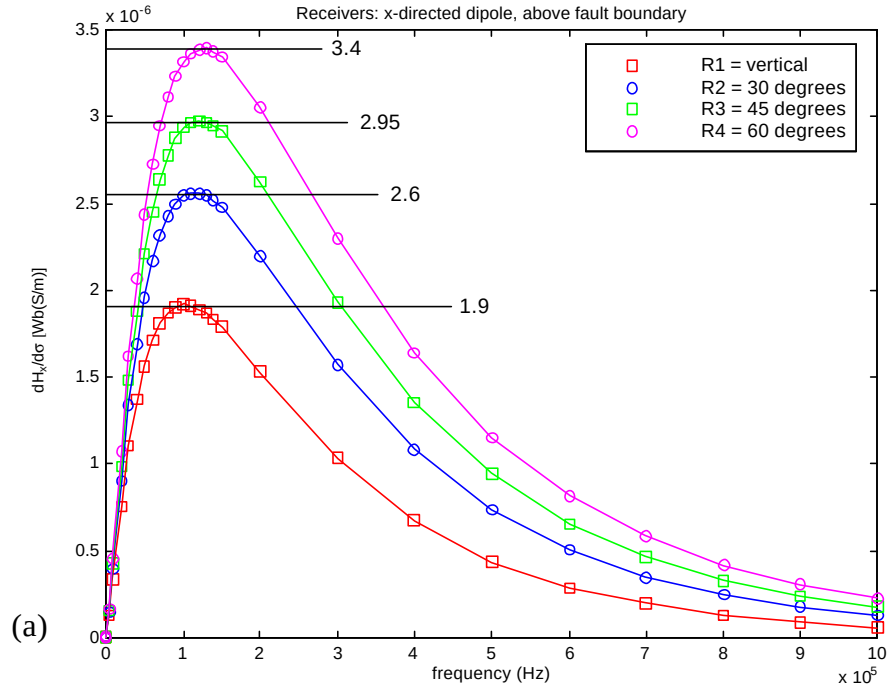

(a)

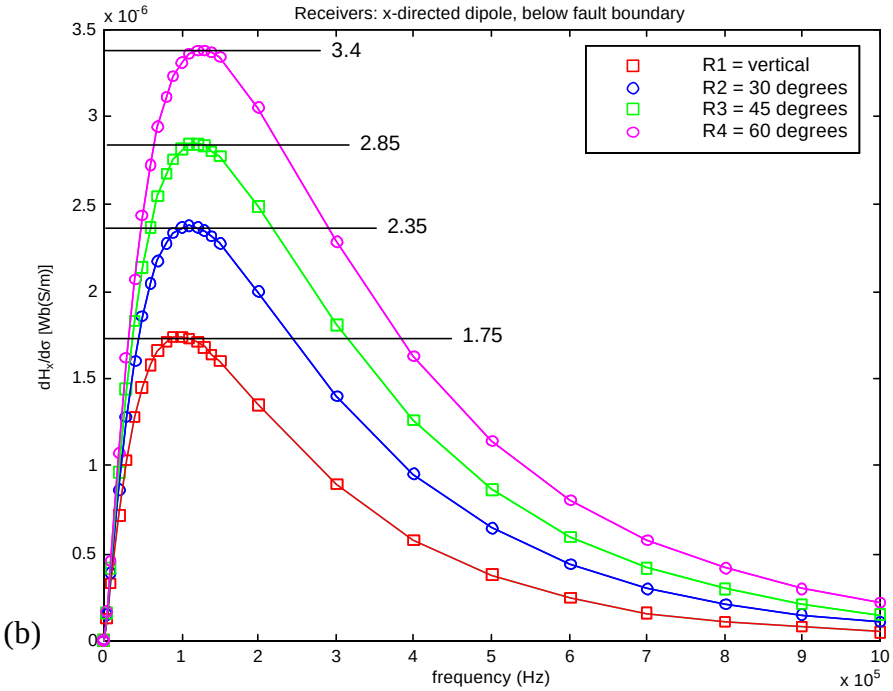

(b)

Figure 3: Sensitivities in the frequency domain for the transmitter and the receivers above (a) and below (b) the fault boundary.

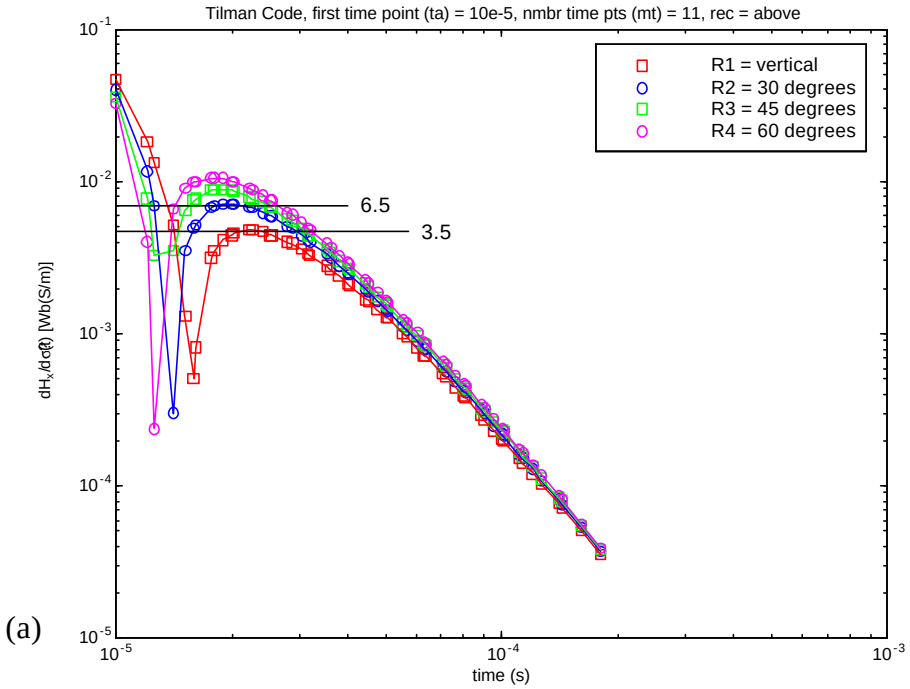

(a)

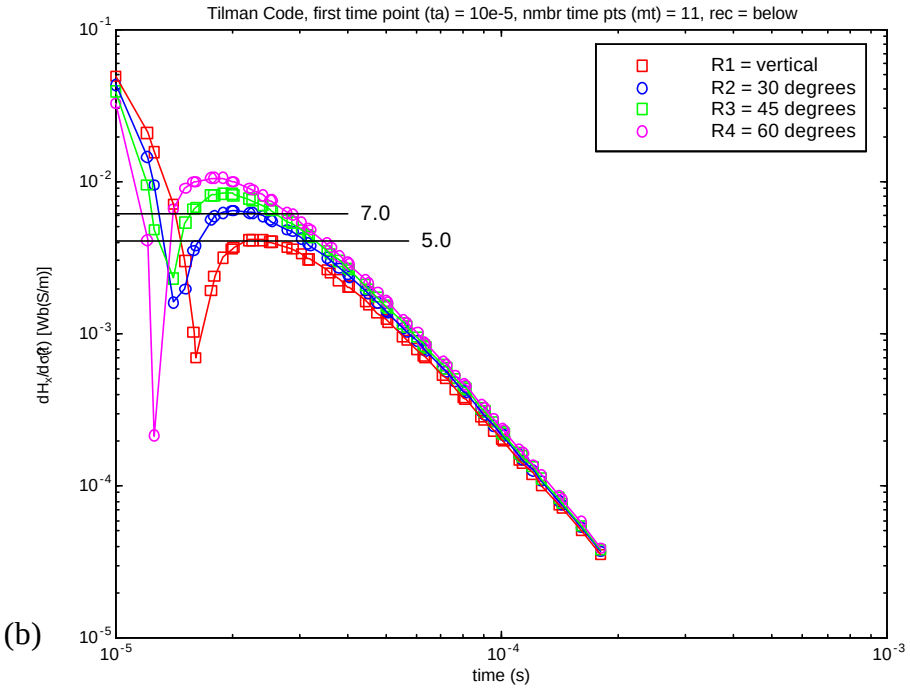

(b)

Figure 4: Time domain sensitivity plots for the transmitter and the receivers above (a) and below (b) the fault boundary.

Distribution:

Dr. Harold Tobin
Department of Earth and Environmental Science
New Mexico Tech
Socorro, NM 87801

1	MS 0750	Marianne C. Walck	(06116)
1	MS 0750	Chester J. Weiss	(06116)
1	MS 0750	Nancy H. Natek	(06116)
1	MS 0750	Lewis C. Bartel	(06116)
1	MS 1088	Gerald L. Peace	(06116)
1	MS 0899	Technical Library	(09616)
1	MS 9018	Central Technical Files	(08945-1)